IEEE Access
Multidisciplinary | Rapid Review | Open Access Journal

Received 14 February 2023, accepted 25 February 2023, date of publication 6 March 2023, date of current version 14 March 2023.

Digital Object Identifier 10.1109/ACCESS.2023.3253563

RESEARCH ARTICLE

Dielectric Modulated Bilayer Electrode Top Contact OTFT for Label Free Biosensing

SUSHIL KUMAR JAIN[1], AMIT MAHESH JOSHI[1], (Senior Member, IEEE), AND LINGA REDDY CENKERAMADDI[2], (Senior Member, IEEE)

[1]Department of ECE, Malaviya National Institute of Technology Jaipur, Jaipur 302017, India
[2]Department of Information and Communication Technology, University of Agder, 4879 Grimstad, Norway

Corresponding author: Linga Reddy Cenkeramaddi (linga.cenkeramaddi@uia.no)

This work was supported in part by the Ministry of Electronics and Information Technology, India, under Visvesvaraya Scheme for Ph.D.; and in part by the Indo–Norwegian Collaboration in Autonomous Cyber-Physical Systems (INCAPS) of International Partnerships for Excellent Education, Research and Innovation (INTPART) Program from the Research Council of Norway under Project 287918.

ABSTRACT In this paper, dielectric modulated bilayer electrodes top contact organic field effect transistor (DMBETC-OTFT) is investigated as a biosensing device for label-free detection of biomolecules. The nanocavity used for biomolecule detection is created by etching the oxide in a conventional OTFT device. Neutral and charged biomolecules can be detected by the proposed device using their respective dielectric constants and charge densities. Subthreshold swing (SS), on-current (I_{ON}), and on-off current ratio (I_{ON}/I_{OFF}) are the main biosensing performance characteristics computed and compared for different gate work function (ϕ_m) and cavity thickness (T_{gap}) for the proposed biosensor device. The change in drain current (I_D), as well as the I_{ON}/I_{OFF} ratio, have both been calculated to investigate the sensitivity of the proposed biosensor. The influence of the gate work function is also investigated to improve the sensitivity of the proposed device. According to the finding of this study, using a gate work function with a lower value results in a significant increase in sensitivity. For charged biomolecules ($Q_f = +1 \times 10^{12} cm^{-2}$) with dielectric constant of biomoecules (K = 12), the highest drain current sensitivity is 4.5×10^3. The drain current sensitivity achieved is four times greater, when comparing the proposed device to the latest published work of metal controlled dielectric modulated OTFT-based sensor. The proposed device also has a high I_{ON}/I_{OFF} sensitivity of 4.60×10^2 when $V_{GS} = -3.0$ V and $V_{DS} = -1.5$ V. In light of its high sensitivity, low cost, and bio-compatibility, the DMBETC-OTFT biosensor holds great promise for the advancement of new demanding flexible biosensing applications.

INDEX TERMS Biosensor, dielectric, OTFT, sensitivity, simulation.

I. INTRODUCTION

Biosensors have the possibility of becoming an effective tool for early illness identification and treatment, thereby lowering the cost of medical treatments for patients. To minimize complications at a later stage, it is helpful to give better point-of-care services in cases of critical illness [1], [2], [3], [4], [5]. Biosensors can be broadly divided into two categories based on their detection methods: labeled detection and label-free detection. In biosensors, chemiluminescence, fluorescence, and radioactivity are popular label detection approaches [6]. Unlike labeled detection, label-free detection does not need a secondary entity for bio-recognition. Label-free detection is particularly used in surface plasmon resonance (SPR), acoustic waves, mass spectrometers, and electrochemical biosensors [7]. Label-free electrochemical biosensors use transducers to convert biomolecule interactions into electrical signals. field-effect transistors (FETs) have the potential to directly convert bio-interactions into readable signals as a transducer, making them promising biosensors. The ability of FET-based, label-free biosensors to identify biological species has received extensive coverage in the literature.

The associate editor coordinating the review of this manuscript and approving it for publication was Santosh Kumar.

A field-effect transistor (FET) based biological applications have expanded significantly [8]. Dielectric modulated FET-based biosensing was utilized to detect COVID-19, a highly contagious coronavirus disease [9]. There are mainly two basic types of biomolecules, which are as follows: i) neutral biomolecules; ii) charged biomolecules. Ion-sensitive field effect transistors (ISFETs) have difficulty identifying neutral biomolecules, so researchers came up with the concept of a dielectrically modulated field effect transistor (FET) biosensor. In this type of biosensor, a cavity area in the oxide dielectric layer is utilized for biomolecule sensing [10]. This is possible because the immobilization of biomolecules in the cavity causes a change in the effective gate capacitance of the proposed device. Various research groups [11], [12], [13], [14], [15], [16] have discussed the utility of FET-based dielectrically modulated biosensors. The literature contains several types of dielectric modulated biosensors, including nanosheet gate all around FETs [17], organic FETs [18], carbon nanotube FETs [3], tunnel FETs [19], and impact ionization FETs [20].

FETs based biosensors can be made from both inorganic and organic semiconducting materials [13], [18]. FET-based biosensors using inorganic semiconductors like silicon have shown several benefits, including compatibility with CMOS technology and inexpensive label-free detection. However, the fabrication of inorganic semiconductor-based electronic devices necessitates expensive patterning, high temperatures, and vacuum deposition [21], [22]. Organic thin film transistors (OTFTs) are created using organic semiconductors, which are an alternate semiconductor material [4]. These substances may be used with stretchy, biocompatible, and flexible substrates. Since organic semiconductors can be processed at temperatures below 100°C, they may be used to fabricate electronic devices on flexible and plastic substrates. Since organic semiconductors can be dissolved in common solvents, they may be typically processed from solutions using simple techniques like roll-to-roll printing, which keeps production costs down. Costs for fabricating biosensors based on OTFT technology can be reduced significantly [23]. Because of their simplicity of fabrication and lesser cost, OTFTs seem to be a good choice for usage in biosensors, especially when where one-time use, biodegradable, inexpensive, and disposable devices with accurate output are required. Poly(3-hexylthiophene), dinaphtho[2,3-b:2',3'-f]thieno[3,2-b]thiophene (DNTT), Poly(3,4-ethylenedioxyselenophene) (PEDOS), and pentacene are the popular organic semiconducting materials, used to create organic thin-film transistors (OTFTs) [22]. Biosensing applications have made great use of them [24].

Rashid et al. [18] have investigated the dielectrically modulated label-free metal trench dielectric modulated OTFT as a biosensor. Recent studies have revealed that OTFT-based dielectrically modulated biosensors are highly helpful in detecting a wide range of biomolecules like streptavidin, biotin, protein, gelatin, and DNA [18]. The literature on dielectric-modulated OTFT-based biosensors is limited in terms of simulation and modeling efforts than the inorganic dielectric-modulated FET-based biosensors. Researchers are still trying to get high sensitivity using OTFT-based biosensors. So, a novel dielectric-modulated OTFT-based biosensor with improved sensitivity is investigated in this work. DNTT is used as an organic semiconducting material in the proposed OTFT-based biosensor. DNTT is the most resistant organic semiconductor to chemical decomposition, high temperatures, oxidation, and defect state generation [25]. The proposed biosensor has bilayer electrodes to improve the performance of the device. After introducing an appropriate metal oxide layer (TiO_2) between the organic semiconductor and gold electrodes, the barrier height can be reduced significantly, improving device performance [26]. To implement label-free biosensing, a cavity is created within the dielectric layer of the OTFT. Because of the inclusion of biomolecules, the dielectric permittivity of the cavity would shift, which causes a variation in the gate capacitance. Finally, a new biosensing device called the dielectric modulated bilayer electrode top contact organic thin film transistor (DMBETC-OTFT) for label-free biosensing has been proposed. Modulation of the dielectric constant during the sensing process for neutral or weakly charged biomolecules (biotin, streptavidin, and protein) occurs when biomolecules with varying dielectric constants are present in the cavity. The charge (Q_f) and dielectric constant (K) modulation effects determine the sensitivity of the dielectrically modulated OTFT-based biosensor for highly charged biomolecules like DNA. The novel contributions in this paper are:

- The proposed DMBETC-OTFT has four times better performance than the most recently reported article based on a metal trench OTFT biosensor [18] for sensing biomolecules.
- To the best of our knowledge, this is the first attempt at a detailed performance analysis of the DNTT-based DMBETC-OTFT biosensor. A novel device structure for a biosensing application is analyzed using rational simulation theory.
- The proposed biosensor is also examined to see how the gate work function (ϕ_m) and fill factor (FF) affect its sensitivity. Through optimization of the gate work function, the DMBETC-OTFT biosensor achieves significant improvements in both the drain current sensitivity and the I_{ON}/I_{OFF} sensitivity.
- To improve the sensitivity of the biosensor, bilayer contacts (TiO_2/Au) are used. Because, in comparison to bare metal electrode devices in conventional OTFT, OTFT devices with an oxide interlayer exhibit a reduced injection barrier and higher performance.
- Because of its simpler fabrication, flexibility, low cost, and biocompatibility, the DMBETC-OTFT biosensor offers significant promise for future flexible electronics.

The investigated design of DMBETC-OTFT based biosensor provides high performance. The proposed biosensor has

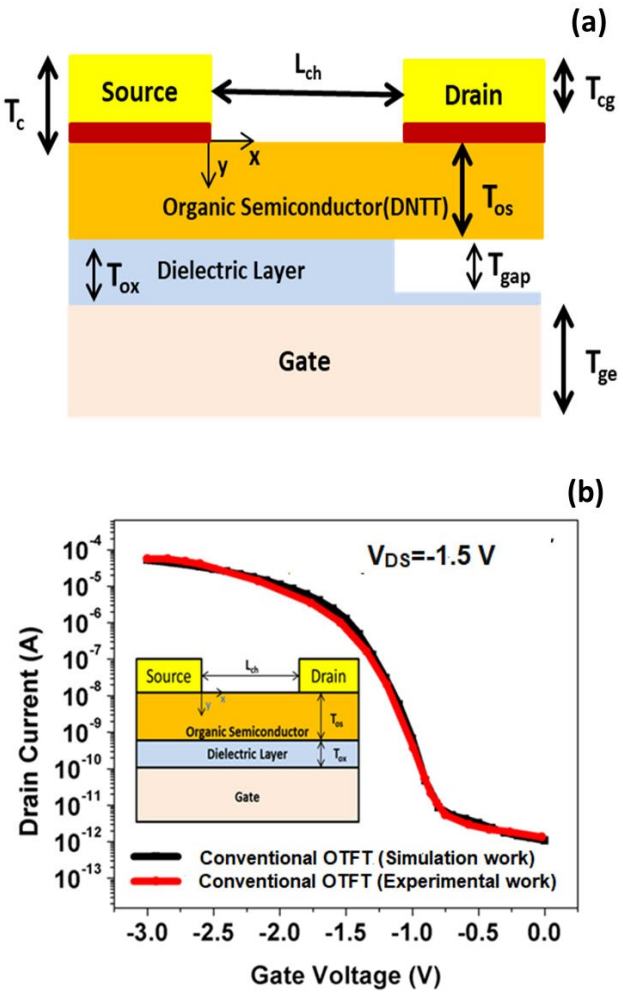

FIGURE 1. (a) DMBETC-OTFT biosensor structure (b) TCAD calibration by matching the experimental characteristic [27] to simulated characteristics.

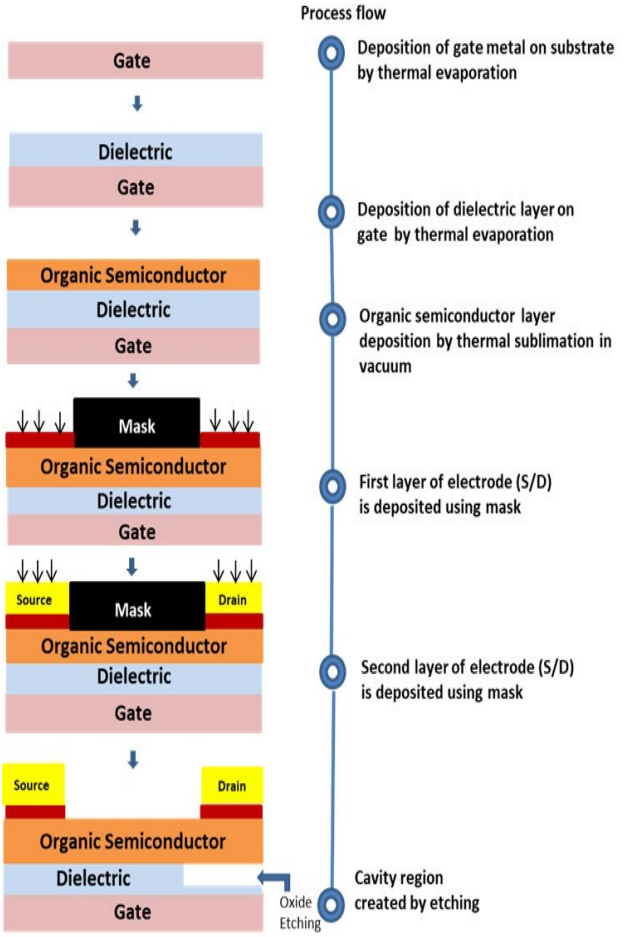

FIGURE 2. Flowchart for the fabrication process of a proposed DMBETC-OTFT-based biosensor.

great potential for future applications in flexible label-free biosensing and pushes the boundaries of OTFT for flexible biochips. The remaining sections of this paper are as follows: Section II discusses the structure, operation, and simulation theory of the proposed biosensor. Section III outlines the biosensor fabrication process. Section IV details the results and findings. The conclusions are provided in section V.

II. DEVICE STRUCTURE, OPERATION & SIMULATION THEORY

A. DESIGN PARAMETERS OF PROPOSED DEVICE

Fig. 1(a) depicts a diagram of the proposed dinaphtho[2,3-b:2',3'-f]thieno[3,2-b]thiophene (DNTT)-based DMBETC-OTFT device, and Table 1 reports the simulation parameters. The proposed design employs DNTT material as an organic semiconductor with a bilayer source and drain electrodes (TiO_2(5 nm)/Au(20 nm)) to improve the performance and sensitivity of the proposed biosensor over a traditional OTFT biosensor [26]. The cavity area in the oxide dielectric layer is created for biomolecule recognition. The bandgap of DNTT is considered to be 3.38 eV [25], the electron affinity of DNTT is given to be 1.81 eV [25], and the relative permittivity of DNTT is taken to be 3.0 [24], [25]. The thickness of the etched cavity in the dielectric oxide layer varies from 10 nm to 5 nm because the thickness of the biomolecules being studied like biotin, streptavidin, and DNA lies in the 10 nm range [10], [28]. The gate oxide dielectric constant is assumed to be 3.37 [27]. The work function of the gate material altered from 4.28 eV (aluminum) to 3.91 eV (hafnium) to maximize device sensitivity. The bilayer gold and TiO_2 electrode for source and drain have work functions of 5.0 eV [29] and 5.4 eV [30], respectively.

B. OPERATION

In label-free electrochemical biosensors, electrochemical transducers translate biomolecule interactions into electrical signals. The proposed dielectric-modulated OTFT converts biomolecule interaction in the OTFT cavity area into a measurable shift in drain current, current I_{ON}/I_{OFF} ratio, or other electrical parameters. Chemi-resistive transduction is used in dielectric-modulated OTFT-based biosensors to change the drain current by changing the transistor surface

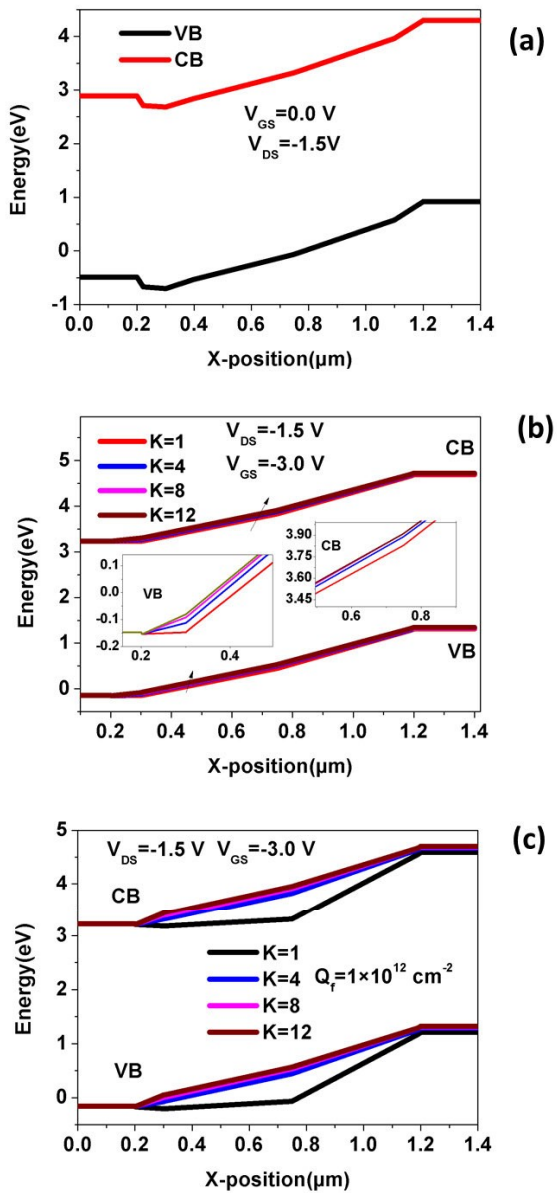

FIGURE 3. HOMO-LUMO Band presentation of DMBETC-OTFT in (a) OFF-state (b) ON state (for neutral biomolecules) (c) ON state (for charged biomolecules) along X-position.

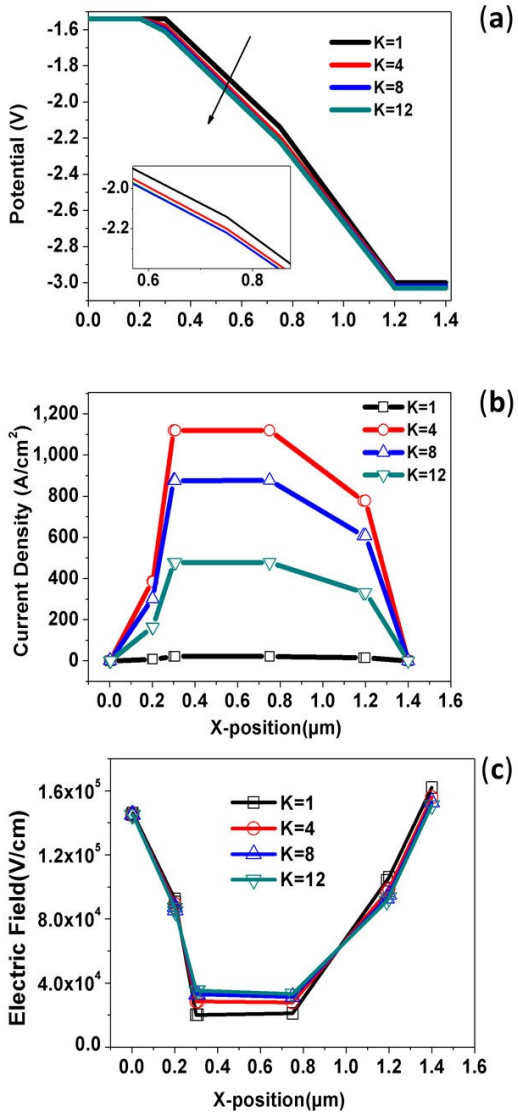

FIGURE 4. For different dielectric constants (a) potential profile (b) current density profile (c) electric field variation, along X-position.

potential due to biomolecule immobilization in the cavity area. The presence of biomolecules in the cavity changes the effective capacitance. When the gate capacitance of the device changes, it enhances the gate control over the source-to-channel junction. This increases the electrostatic control of the gate over the junction. As a biomolecule transducer, dielectrically modulated OTFT has the potential to convert bio-interactions into readable signals, making them promising biosensors.

TABLE 1. Device parameter used in simulation.

Symbol	Name of Parameter	Value
T_{os}	active layer (DNTT) thickness	25 nm
E_g	DNTT HOMO-LUMO energy gap	3.38 eV
χ	DNTT electron affinity	1.81 eV
ϵ_r	DNTT relative permittivity	3.0
T_{gap}	thickness of cavity region	10 nm to 5 nm
ϵ_{ox}	dielectric constant of oxide	3.37
T_{ox}	thickness of dielectric	12.3 nm
T_c	total thickness of contacts (Source/Drain)	30 nm
T_{ge}	thickness of gate electrode	30 nm
L_{ch}	length of channel	1μm
ϕ_{TiO_2}	TiO_2 electrode work function	5.4 eV
ϕ_{Au}	gold electrode work function	5.0 eV
ϕ_m	gate work function	3.91 eV to 4.28 eV

C. SIMULATION APPROACH

The behavior of electronic devices can be predicted and optimized using simulators with a thorough understanding of device physics before the actual fabrication. Silvaco Atlas 2-D numerical device simulator, a benchmarked industry

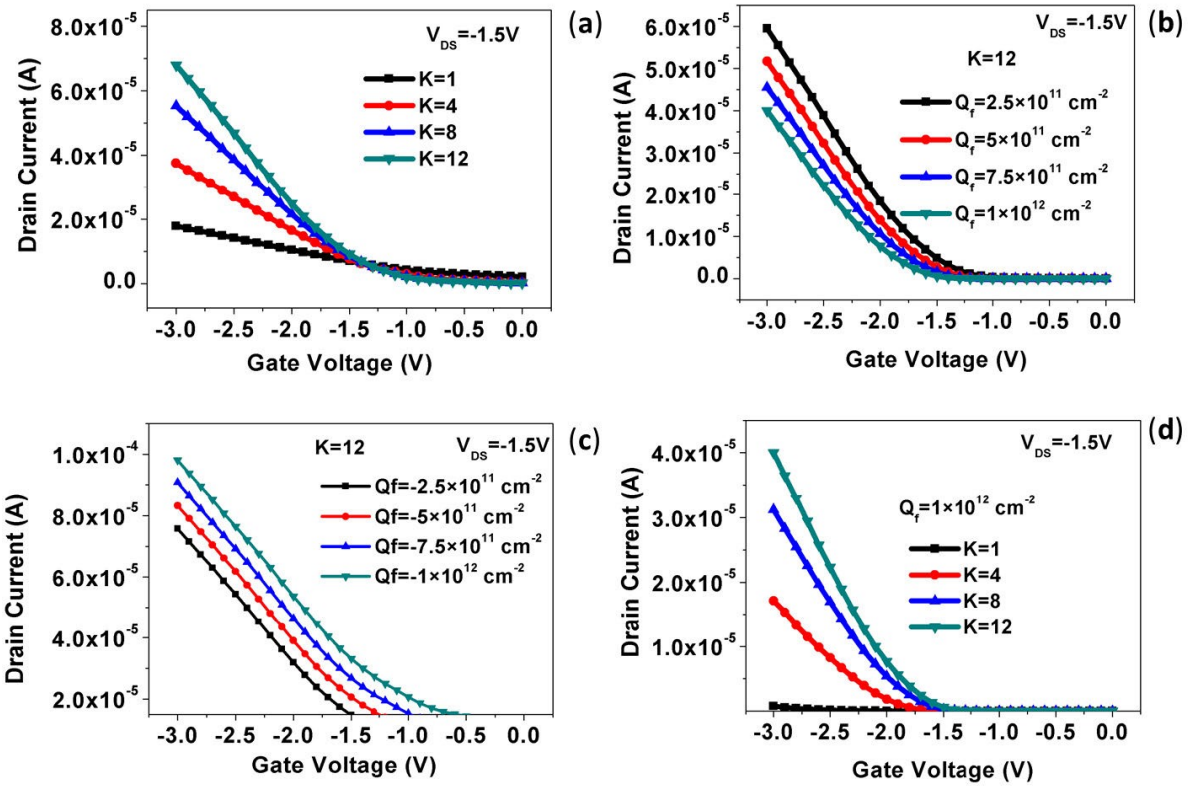

FIGURE 5. Characteristics (Transfer) of proposed for (a) biomolecules having no charge (neutral) (b) biomolecules having positive charge density (c) biomolecules having negative charge density and (d) fix charged biomolecules ($Q_f = +1 \times 10^{12} cm^{-2}$) with varying K, at $V_{DS} = -1.5$ V.

standard, is used to analyze the performance of the proposed structure. To explore the behavior of the proposed device, the structure is often transformed into a grid of finite elements. The simulator solves discrete fundamental equations like Poisson and Continuity equations [29] based on device physics at each location in the simulation domain to analyze the performance of the device.

Atlas simulation generally has three steps [31]:

1) Mesh and structural specification: The several simulation domains are then divided into a finite element grid form termed "mesh," which consists of a complex grid of triangles, once all of the proposed OTFT layers have been created with the requisite dimensions. At each discrete grid point, the model demands computations based on elemental device physics equations. A meshing grid with a high node density can be used to obtain a high level of accuracy. Despite this, it employs a finite element technique and necessitates a substantial level of convergence in both the device simulation and the circuit realization.
2) Physical models and material parameters: In this section, physical models and material parameters are defined. The density of defect states model and the Poole-Frenkel mobility model [31] are both utilized in the simulation of the proposed OTFT-based biosensing device. These models can show the conduction that occurs as a result of the electric field-dependent thermal activation of trapped charge carriers.
3) Biasing condition: This section is responsible for defining the bias conditions applicable for simulation, which may include gate voltage and drain voltage, to specify the electrical properties of the proposed device. When evaluating the performance of the proposed structures, electrical properties, and parameters are taken into consideration.

Before the Investigation, calibration of the TCAD model is done by matching the transfer characteristics of the experimental data [27] to the simulation results as presented in Fig. 1(b).

III. FABRICATION PROCESS FLOW

Fig. 2 shows the process of fabrication of the proposed biosensor. The steps involved in making an OTFT have been described in detail by several researchers [27], [31], [32]. The DMBETC-OTFT-based biosensor can be fabricated using the same methods as traditional nanogap OTFT biosensors. Thermal evaporation deposits aluminum as a gate electrode layer on a substrate, the gate dielectric formed by native oxide is increased by a short exposure to oxygen. The organic semiconductor is then thermally sublimated in a vacuum at

TABLE 2. Dielectric constant (K) of various biomolecules.

Name of Biomolecule	K	References
biotin	2.63	[33]
streptavidin	2.1	[11]
APTES	3.57	[11]
protein	8.0	[11]
DNA	6	[11]
gelatin	12	[14]

60°C. Stencil masks were used to deposit the bi-layer of the source and drain contacts onto the semiconducting layer. Finally, the wet etching method can be used to etch the oxide from the drain side to create the cavity for biomolecules.

IV. RESULTS AND DISCUSSIONS

Environmental biomolecules may be neutral or charged. When modeling the impact of a biomolecule on performance parameters, just the dielectric constant is needed for a neutral molecule, while the dielectric constant and charge density are needed for a charged molecule. This proposed sensor is capable of detecting neutral biomolecules with various dielectric constants, including streptavidin, which has K = 2.1 (used for nucleic acid and lipid detection), protein, which has K = 8 (required for tissue repair), and biotin, which has K = 2.63 (which controls blood sugar) [11]. This biosensor can also be used to detect charged biomolecules like DNA, which have a range of dielectric constants of K = 1 to 64 [10]. However, K = 6 is a typical value for the dielectric constant of DNA [11]. The literature revealed that the charge density (Q_f) of charged biomolecules like DNA ranges from $-1 \times 10^{11} cm^{-2}$ to $+1 \times 10^{12} cm^{-2}$ [12], [14]. Table 2 provides biomolecule dielectric constants. When biomolecules are present in the device, the effective gate capacitance is different from when the cavity is empty. Because the biomolecule having a dielectric constant (K > 1) is present in the cavity area, the effective gate capacitance goes up. This changes the conduction current density of the channel because the gate and channel are coupled in the cavity area.

A. HOMO-LUMO BAND DIAGRAM, POTENTIAL, CONDUCTION CURRENT DENSITY & ELECTRIC FIELD PROFILE

To comprehend the physical mechanism, first consider the impact of different biomolecules on the field intensity profile, energy band diagram, conduction current density, and potential profile. The most significant condition for biomolecule conjugation in the cavity area should be observed as band bending in the channel area. First, the influence of the coupling of biomolecules on the HOMO-LUMO energy band diagram of DMBETC-OTFT is examined [34]. HOMO-LUMO band structure in its OFF condition (V_{GS} = 0 V and V_{DS} = −1.5 V) is illustrated in Fig. 3(a), while the band structure in its ON condition (V_{GS} = −3.0 V and V_{DS} = −1.5 V) along the horizontal X-position is depicted in Fig. 3(b) with variable dielectric permittivity for different neutral biomolecules. Fig. 3(c) represents the HOMO-LUMO energy band structure for the proposed biosensor in its ON condition (V_{GS} = −3.0 V and V_{DS} = −1.5 V). Band bending occurs when the biomolecules having K >1 are attached in the cavity region. Band bending at HOMO and LUMO levels occurs due to changes in gate capacitance after the coupling of biomolecules in the cavity. It can be seen from Fig. 3(b)-(c) that increasing K of the biomolecules causes additional band bending, which decreases the barrier width even further due to a change in gate capacitance. The band diagram study reveals that band bending narrows the space between barriers as the dielectric constant grows.

Fig. 4(a) depicts the potential profiles of several biomolecules with changing dielectric constants. The improved capacitive behavior optimizes the distribution of the potential profile. When biomolecules are missing in the nanogap cavity area, the surface potential level is at its lowest (K = 1 for air). The operation of the proposed biosensor is operated possibly by a mechanism known as chemo-resistive transduction. A result of biomolecule immobilization in the cavity causes a change in the potential profile of the proposed sensor. This change in surface potential affects the drain current that is flowing through the device. As shown in Fig. 4(b), when the biomolecules of larger dielectric constants immobilize, more carriers are in the channel area, which makes the conduction current density swing up. A change is brought about in the current density distribution of the device as a result of the immobilization of a variety of biomolecules in the nanogap area of the oxide layer. The increase in the dielectric constants of the biomolecules results in an even greater increase in the value of the current density that is already present in the channel. This occurs as a result of the proportional relationship between the K of biomolecules and the gate capacitance of the device. Finally, variations in the conduction current density in the channel area would directly affect the magnitude of the drain current flowing through the proposed device. When the dielectric constant of biomolecules reaches its maximum value, which is denoted by the K = 12, the conduction current density reaches its greatest value. Fig. 4(c) shows the pattern of field intensity strength for different dielectric constants resembling biomolecules. The largest electric field intensity is found for a biomolecule having K = 12, indicating a higher degree of barrier modification to allow carrier transit. In contrast, the smallest electric field is found for a molecule with K = 1.

B. IMPACT OF BIOMOLECULES IMMOBILIZATION ON DRAIN CURRENT

Based on the results shown in Fig. 5(a), the on-current (I_{ON}) gets higher as the biomolecules in the cavity area have a higher dielectric constant. This happens because the dielectric constant of biomolecules rises, which causes the effective gate capacitance to increase. Since the drain current is proportional to its capacitance, it makes sense that as K of the biomolecules gets higher, so will the drain current. This shows that an increase in K makes the capacitive property better. Fig. 5(b) and 5(c) show how the binding of different

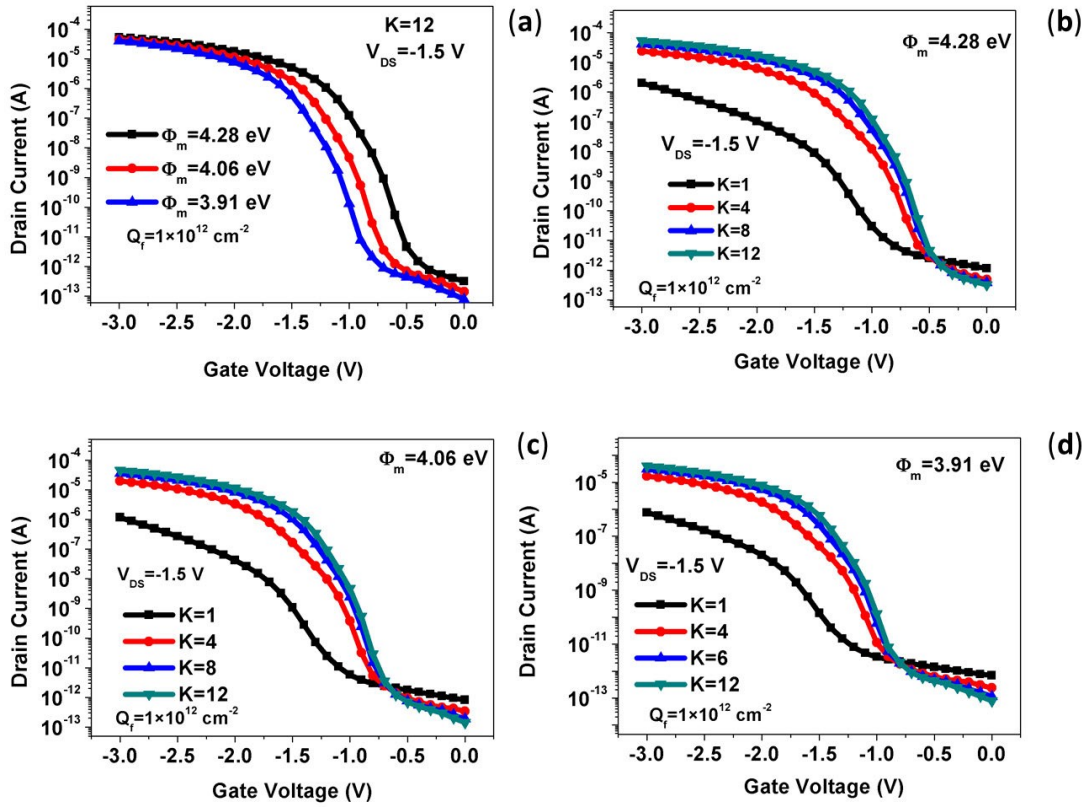

FIGURE 6. Gate work function (ϕ_m) effect on electrical characteristics (a) for varying ϕ_m and K = 12 (b) for ϕ_m = 4.28 eV and varying K = 1 to K = 12 (c) for ϕ_m = 4.06 eV and varying K = 1 to K = 12 (d) for ϕ_m = 3.91 eV and varying K = 1 to K = 12.

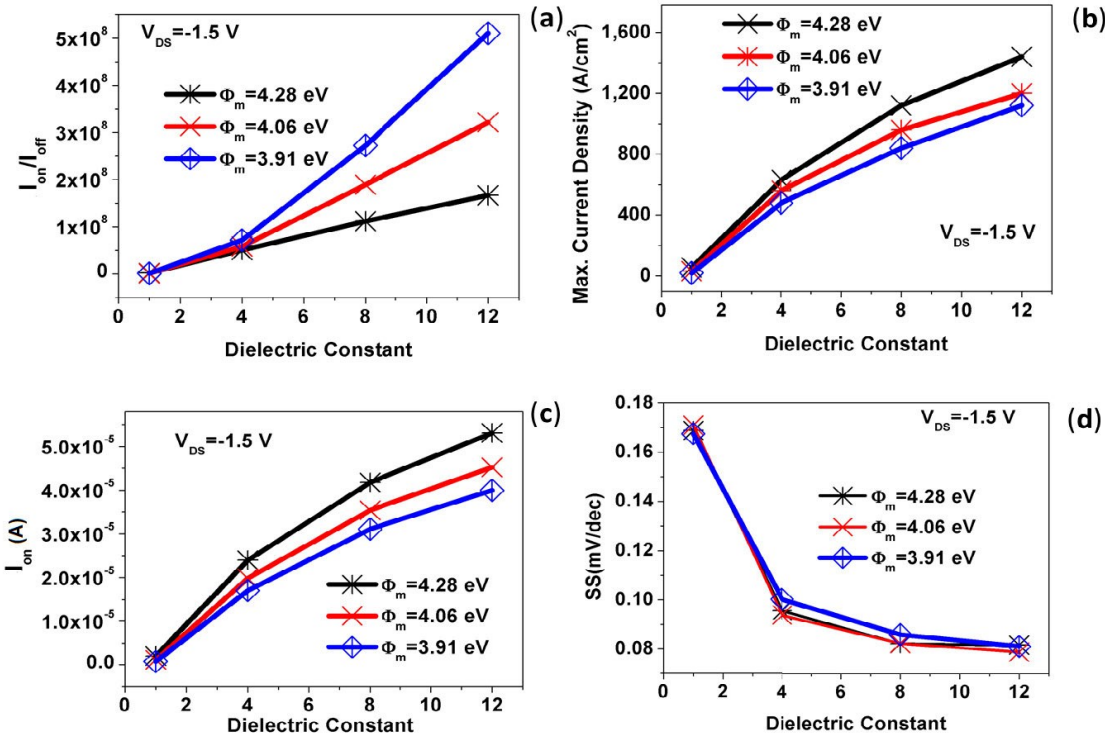

FIGURE 7. Impact of the varying work function of the gate (ϕ_m) at $V_{DS} = -1.5$ V on (a) I_{ON}/I_{OFF} ratio (b) density of conduction current (c) on-current (I_{ON}) (d) subthreshold swing (SS).

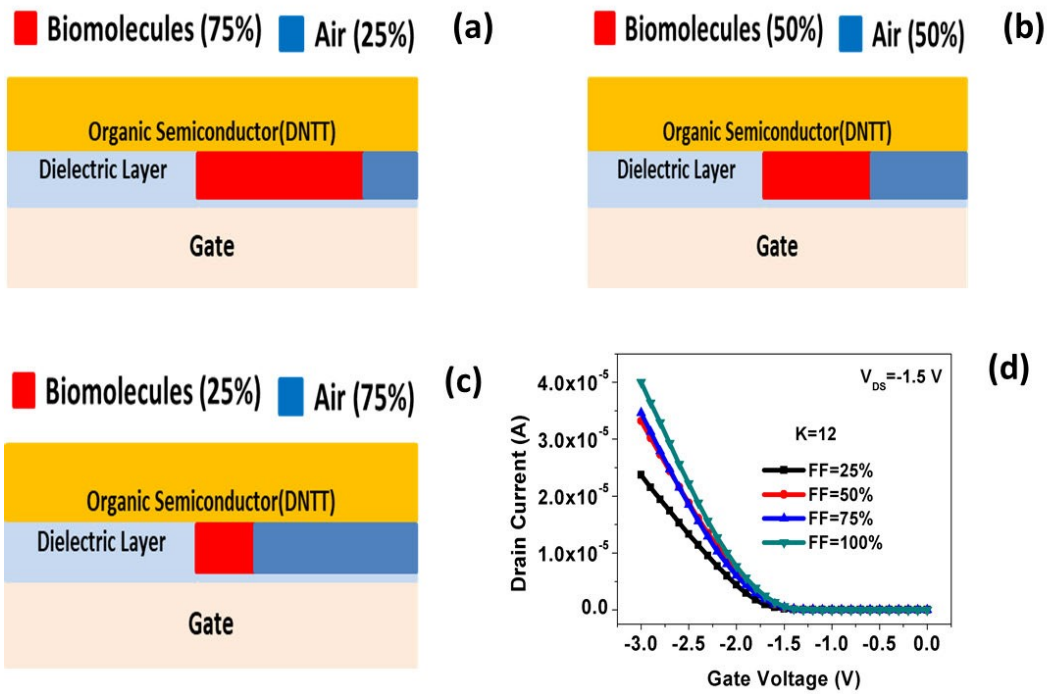

FIGURE 8. (a)-(c) Fill factor representation for different quantity of biomolecules in the cavity (d) transfer characteristic for different values of fill factor.

positively and negatively charged biomolecules changes the transfer characteristic with K = 12 and a cavity thickness (T_{gap}) of 10 nm. This change is shown when the voltage is $V_{DS} = -1.5$ V. When there is a greater charge density of negative charges on biomolecules, the on-current (I_{ON}) rises due to variation in accumulation of charges. But, the on-current (I_{ON}) decreases due to an increase in the magnitude of positivity charge density associated with biomolecules. The threshold voltage is significantly affected due to the charge modulation in the cavity area. Due to charged biomolecule interaction, threshold voltage alters the magnitude of the drain current. When the biomolecules having constant charge density ($Q_f = +1 \times 10^{12} cm^{-2}$) but variable dielectric constant (K = 1 to 12) binds in nanogap area, the significant variation in magnitude of on-current (I_{ON}) occurs as shown in Fig. 5(d). The drain current varies greatly at K = 12 due to larger capacitance for a high dielectric constant.

C. ELECTRICAL CHARACTERISTICS FOR DIFFERENT GATE WORK FUNCTION (ϕ_m)

The effect on the electrical characteristics of the proposed biosensor for different gate work functions (ϕ_m) is explained in this section. The variation in transfer characteristics of the proposed biosensor coupled with charged biomolecules (K = 12 and $Q_f = +1 \times 10^{12} cm^{-2}$) using different gate work functions is depicted in Fig. 6(a). The injection barrier at the source-drain junction starts to reduce as the value of the work function of the gate material is raised. The drain current increases as a result of a lower injection barrier, which is caused by a larger work function of the gate material. Fig. 6(b)-(d) exhibits the properties of the biosensor in the presence of biomolecules with K values of 4, 8, and 12 at gate work function (ϕ_m) values of 4.28 eV, 4.06 eV, and 3.91 eV, respectively. Changes in the work function of the gate material affect the electrostatic gate control of charge carrier injection. Changes in the gate work function (ϕ_m) have a substantial effect on the electrical properties of the proposed biosensor. Fig. 7(a) shows the changes of I_{ON}/I_{OFF} ratio with change of gate work-function (ϕ_m) changes. Fig. 7(b)-(c) shows that the current density and on-current(I_{ON}) of the proposed sensor rise at a higher work function of the gate, indicating a decrease in charge carrier injection. Subthreshold swing (SS), as shown in Fig. 7(d), minimally shifts when the gate work function (ϕ_m) changes from 4.28 eV to 3.91 eV. Performance characteristic, I_{ON}/I_{OFF} ratio is greatly enhanced by reducing the gate work function (ϕ_m) to a smaller value. The current on-off ratio is at its highest when the work function is at its lowest. This is because the gate work function has a significant impact on the threshold voltage. Threshold voltage directly affects the off current of the device, and this effect is mirrored by changes in the I_{ON}/I_{OFF} ratio. The subthreshold swing of the device stays relatively the same regardless of the change in the work function of the gate.

D. FILL FACTOR EFFECT ON PERFORMANCE OF BIOSENSOR

Fig. 8(a)-(c) depicts a cavity that is partially filled with biological molecules (25%, 50%,& 75%), and the remaining

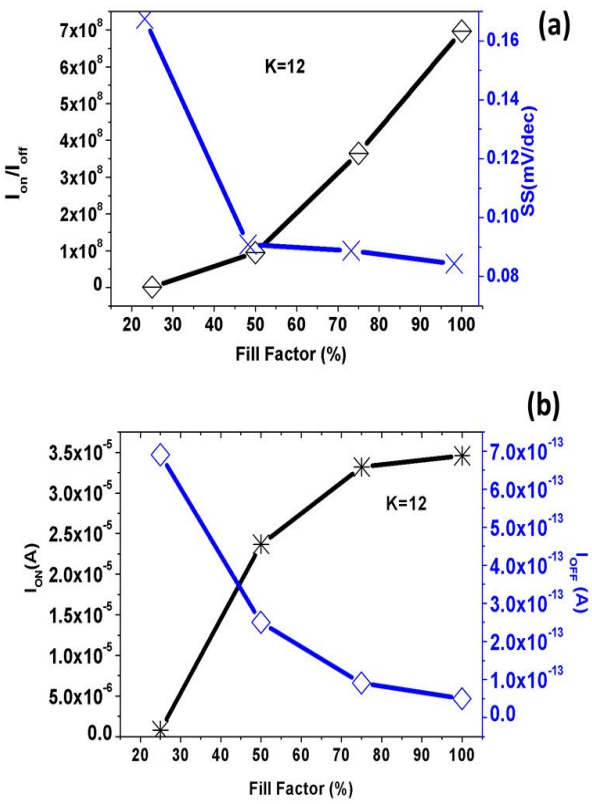

FIGURE 9. Fill factor (FF) influence on (a) subthreshold swing (SS) and I_{ON}/I_{OFF} ratio. (b) on-current (I_{ON}) and off-current (I_{ON}), for different biomolecules.

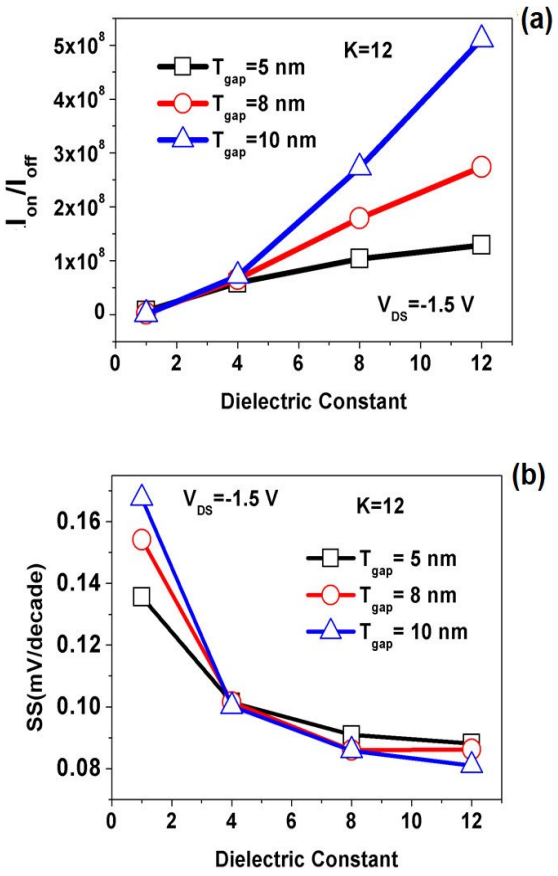

FIGURE 10. Effect of variation in thickness of cavity (T_{gap}) with varying K on (a) I_{ON}/I_{OFF} ratio (b) subthreshold swing (SS).

TABLE 3. Drain current sensitivity comparison with published work.

Ref.	V_{DS}/V_{GS}(V)	K	Drain Current Sensitivity
[36]	0.5/1.0	8	1.385
[37]	1.0/1.0	10	3.3
[18]	-1.5/3.0	12	12.57
[Present work]	-1.5/3.0	12	50.91

part is filled with air. The cavity space should be full of either air or biological molecules. It had been predicted that biological molecules would fill the cavity, yet several bio tests have confirmed the existence of particular vacant spaces in the cavity region. As a result, we now know that the fill factor (FF) is an additional indicator of sensitivity [35]. The amount to which biological molecules occupy space in the cavity of a proposed biosensing device indicates the fill factor (FF). Comparative performance of four configurations (25%, 50%, 75%, and 100%) are examined based on the area covered by biological molecules in the cavity. Fig. 8(d) shows how the filling factor (K = 12, $Q_f = +1 \times 10^{12} cm^{-2}$) affects the properties of the drain current dependent on the surface area occupied by the biomolecules in cavity region. The electrical properties of the DMBETC-OTFT biosensor shift due to the cavity capacitance shifting with different configurations. The filled cavity has a different effective capacitance than the partially filled cavity. Fig. 9(a) shows how the on-current (I_{ON}) and off-current (I_{OFF}) are varying with the change in the filling factor. An increase in the filling factor (FF) from 25% to 100% causes an increase in the on-current (I_{ON}) and a decrease in the off-current (I_{OFF}) in the cavity area due to varying capacitance of cavity. As shown in Fig. 9(b), the on-off ratio (I_{ON}/I_{OFF}) and the subthreshold swing (SS) both improve with an increase in the fill factor due to the corresponding capacitive shift.

E. IMPACT OF CAVITY THICKNESS VARIATION ON PERFORMANCE PARAMETERS

The small change in the I_{ON}/I_{OFF} ratio for biomolecules (K = 12, $Q_f = +1 \times 10^{12} cm^{-2}$) given with change in cavity thickness (T_{gap}) is demonstrated in Fig. 10(a). The effective capacitance is altered as the thickness of the cavity is brought down from 10 nm to 5 nm. When the effective capacitance of the gate shifts as a result of a change in cavity thickness, there is a corresponding shift in the performance characteristics of the device. Capacitance change also causes a minor change in the sub-threshold swing (SS), which is seen in Fig. 10(b) as a function of the cavity thickness (T_{gap}).

F. ANALYSIS OF SENSITIVITY

Sensitivity analysis is required to measure the performance of biological sensors. The following formula for drain current sensitivity (S_D) represented in (1) calculates how sensitive the proposed device is to drain current variations while

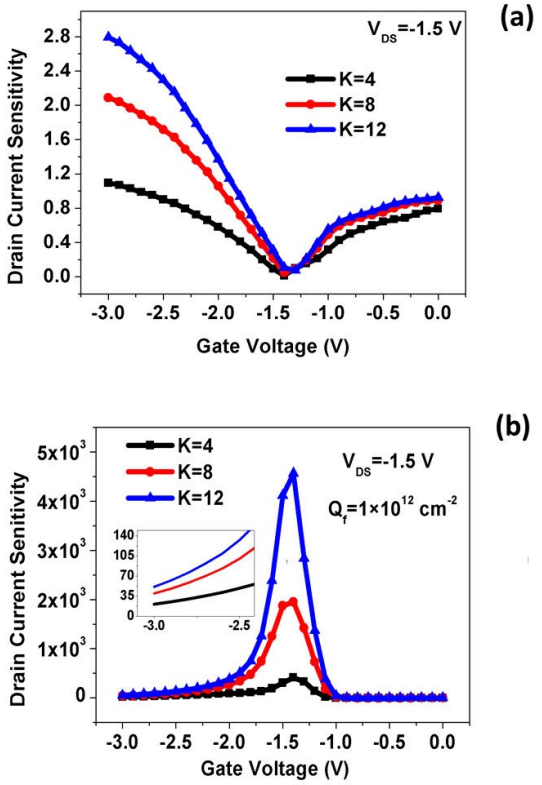

FIGURE 11. (a) Drain current Sensitivity of neutral biomolecules (b) drain current sensitivity of charged biomolecules.

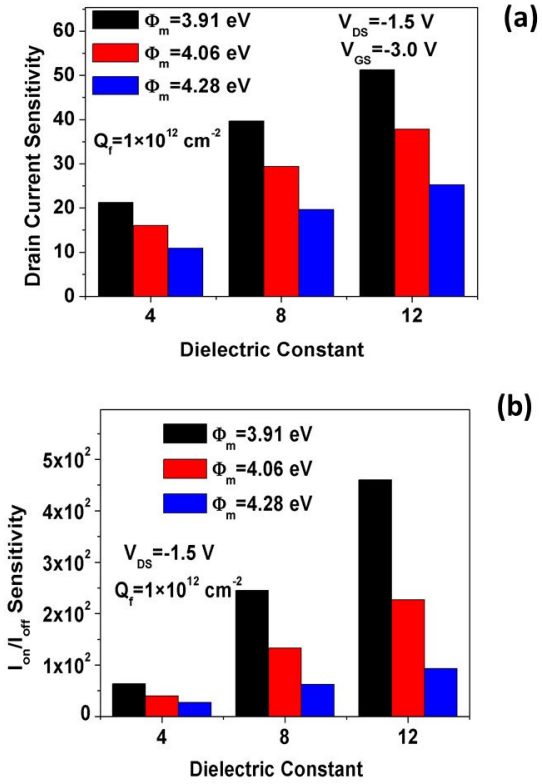

FIGURE 12. Sensitivity analysis with the varying work function of the gate at T_{gap} = 10 nm (a) drain current sensitivity analysis (b) I_{ON}/I_{OFF} sensitivity analysis.

biomolecules are present in the cavity.

$$S_D = \frac{I_D(bio) - I_D(air)}{I_D(air)} \tag{1}$$

when the biomolecules are absent in cavity, I_D (air) equals drain current. To indicate the absence of biomolecules for calculation of sensitivity K = 1 (air) is used in literature [33]. When biomolecules fill the cavity, I_D (bio) equals the drain current when biomolecules are present in the cavity. Fig. 11(a) shows the sensitivity of the drain current to the gate voltage, for neutral biomolecules with varied dielectric constants. As the relative permittivity of biomolecules increases from K = 4 to K = 12, so does the sensitivity of biosensors. As shown in Fig. 11(b), the drain current sensitivity of charged biomolecules shifts when the relative permittivity is changed at a constant charge density ($Q_f = +1 \times 10^{12} cm^{-2}$). For positively charged biomolecules ($Q_f = +1 \times 10^{12} cm^{-2}$), the maximal drain current sensitivity found with K = 12 is 4.6×10^2. Table 3 shows that the drain current sensitivity of biomolecules with K = 12 is 50.91 at $V_{GS} = -3.0$ V and $V_{DS} = -1.5$ V, approximately four times more than OTFT-based biosensor studies [18]. The variation in dielectric constant causes a rise in the device conduction current density, which in turn causes an increase in the sensitivity for charged biomolecules. Fig. 12(a) illustrates how various biomolecules affect drain current sensitivity at different gate work functions (ϕ_m). At $\phi_m = 3.91$ eV, sensitivity is highest, while at 4.28 eV, it is lowest. Sensitivity rises as gate work function value drops. As evidenced by drain current sensitivity, optimizing the work function increases OTFT biosensor maximum sensitivity. As demonstrated in Fig. 12(b), changes in the ratio of on to off current are expressed as I_{ON}/I_{OFF} sensitivity (S_{IR}) for biomolecules with varying gate work-functions (ϕ_m). The following formula calculates the I_{ON}/I_{OFF} sensitivity presented as:

$$S_{IR} = \frac{I_{ratio}(bio) - I_{ratio}(air)}{I_{ratio}(air)} \tag{2}$$

The I_{ON}/I_{OFF} ratio equals I_{ratio} (bio) when a cavity is completely filled by biomolecules, and it equals I_{ratio} (air) when the cavity region is empty. For a device to detect biomolecules, the magnitude of the sensitivity between I_{ON} and I_{OFF} should be higher, as shown in (2).

The sensitivity of the I_{ON}/I_{OFF} transition is greatest at a work-function (ϕ_m) = 3.91 eV and diminishes at larger (ϕ_m) values (4.28 eV). The sensitivity at $V_{GS} = -3.0$ V and $V_{DS} = -1.5$ V for $\phi_m = 3.91$ eV is 4.60×10^2, while at 4.28 eV, it is only 93.18. DMBETC-OTFT sensors have higher I_{ON}/I_{OFF} sensitivity at reduced gate work-function (ϕ_m). The variation in drain current sensitivity for various biomolecules at varying cavity thicknesses is seen in Fig. 13(a). Several biomolecules are shown here with varied dielectric permittivity (K) values, representing the relation

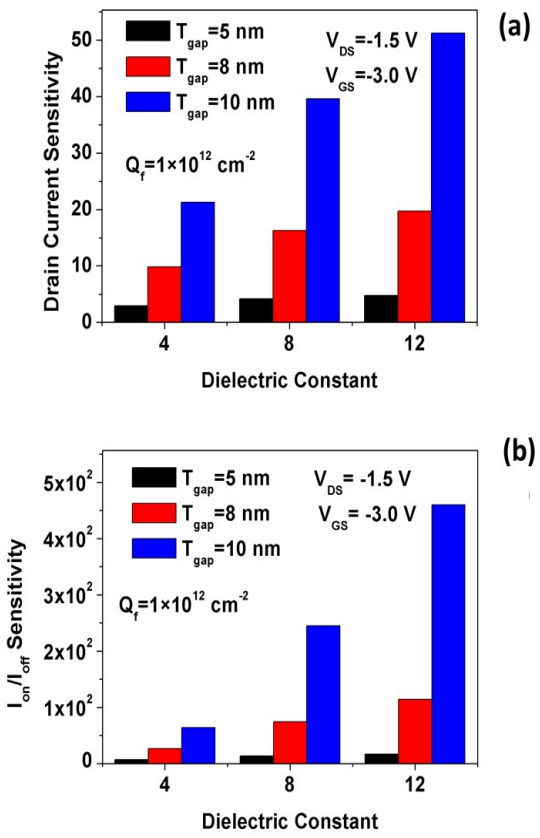

FIGURE 13. (a) Sensitivity analysis with varying thickness of cavity (T_{gap}) (a) drain current sensitivity analysis (b) I_{ON}/I_{OFF} sensitivity analysis.

between drain current sensitivity and these molecules. The optimum sensitivity is attained at a cavity thickness of 10nm (T_{gap} = 10 nm), whereas a thickness of 5 nm yields the minimum sensitivity. Fig. 13(b) illustrates how the I_{ON}/I_{OFF} sensitivity changes with various biomolecules (K = 4, 8, 12) when the cavity thickness is varied. At a thickness of T_{gap} = 10 nm, the sensitivity between is maximized, whereas at a thickness of T_{gap} = 5 nm, the sensitivity is minimized. The sensitivity of the device at $V_{GS} = -3.0$ V and $V_{DS} = -1.5$ V is 4.60×10^2 for $T_{gap} = 10$ nm, while it is only 17.04 for $T_{gap} = 5$ nm.

V. CONCLUSION

Biomolecule sensing is investigated using a DMBETC-OTFT biosensor. First, the influence of several biomolecules on the field intensity profile, energy band diagram, and potential profile is investigated. Subsequently, the changes in (I_{ON}/I_{OFF}) ratio and the on-current (I_{ON}) in response to biomolecules are studied towards the sensitivity analysis of the DMBETC-OTFT based biosensor. The cavity thickness (T_{gap}), fill factor (FF), and gate work function (ϕ_m) were optimized to have a greater sensitivity. DMBETC-OTFT biosensor sensitivity is raised by lowering the gate work function (ϕ_m). The research found that DMBETC-OTFT is four times more sensitive to the detection of biomolecules than recently published metal trench DM-OTFT [18]. As a result, the proposed technology might be employed in the future to create flexible and biocompatible OTFT-based biosensors.

ACKNOWLEDGMENT

The Visvesvaraya Doctoral Scholarship Program of the Indian Government provided some support for this study. The longer version of the paper is archived in [38].

REFERENCES

[1] R. Narang, M. Saxena, and M. Gupta, "Comparative analysis of dielectric-modulated FET and TFET-based biosensor," *IEEE Trans. Nanotechnol.*, vol. 14, no. 3, pp. 427–435, May 2015.
[2] D. Sadighbayan, M. Hasanzadeh, and E. Ghafar-Zadeh, "Biosensing based on field-effect transistors (FET): Recent progress and challenges," *TrAC Trends Anal. Chem.*, vol. 133, Dec. 2020, Art. no. 116067.
[3] S. S. Alabsi, A. Y. Ahmed, J. O. Dennis, M. H. Md Khir, and A. S. Algamili, "A review of carbon nanotubes field effect-based biosensors," *IEEE Access*, vol. 8, pp. 69509–69521, 2020.
[4] C. Sun, X. Wang, M. A. Auwalu, S. Cheng, and W. Hu, "Organic thin film transistors-based biosensors," *EcoMat.*, vol. 3, no. 2, Mar. 2021, Art. no. e12094.
[5] A. M. Joshi, P. Jain, and S. P. Mohanty, "Everything you wanted to know about continuous glucose monitoring," *IEEE Consum. Electron. Mag.*, vol. 10, no. 6, pp. 61–66, Nov. 2021.
[6] A. Syahir, K. Usui, K.-Y. Tomizaki, K. Kajikawa, and H. Mihara, "Label and label-free detection techniques for protein microarrays," *Microarrays*, vol. 4, no. 2, pp. 228–244, Apr. 2015.
[7] S. Mehrabani, A. Maker, and A. Armani, "Hybrid integrated label-free chemical and biological sensors," *Sensors*, vol. 14, no. 4, pp. 5890–5928, Mar. 2014.
[8] Y. C. Syu, W. E. Hsu, and C. T. Lin, "Field-effect transistor biosensing: Devices and clinical applications," *ECS J. Solid State Sci. Technol.*, vol. 7, no. 7, pp. 3196–3207, Jun. 2018.
[9] G. Seo, G. Lee, M. J. Kim, S. H. Baek, M. Choi, K. B. Ku, C. S. Lee, and S. J. Kim, "Rapid detection of COVID-19 causative virus (SARS-COV-2) in human nasopharyngeal swab specimens using field-effect transistor-based biosensor," *ACS Nano*, vol. 14, no. 9, pp. 12257–12258, Apr. 2020.
[10] C.-H. Kim, C. Jung, H. G. Park, and Y.-K. Choi, "Novel dielectric-modulated field-effect transistor for label-free DNA detection," *Biochip J.*, vol. 2, no. 2, pp. 127–134, Jun. 2008.
[11] A. Gedam, B. Acharya, and G. P. Mishra, "Design and performance assessment of dielectrically modulated nanotube TFET biosensor," *IEEE Sensors J.*, vol. 21, no. 15, pp. 16761–16769, Aug. 2021.
[12] M. Verma, S. Tirkey, S. Yadav, D. Sharma, and D. S. Yadav, "Performance assessment of a novel vertical dielectrically modulated TFET-based biosensor," *IEEE Trans. Electron Devices*, vol. 64, no. 9, pp. 3841–3848, Sep. 2017.
[13] C.-H. Kim, J.-H. Ahn, K.-B. Lee, C. Jung, H. G. Park, and Y.-K. Choi, "A new sensing metric to reduce data fluctuations in a nanogap-embedded field-effect transistor biosensor," *IEEE Trans. Electron Devices*, vol. 59, no. 10, pp. 2825–2831, Oct. 2012.
[14] Mahalaxmi, B. Acharya, and G. P. Mishra, "Design and analysis of dual-metal-gate double-cavity charge-plasma-TFET as a label free biosensor," *IEEE Sensors J.*, vol. 20, no. 23, pp. 13969–13975, Dec. 2020.
[15] A. Dixit, D. P. Samajdar, and N. Bagga, "Dielectric modulated GaAs FinFET as a label-free biosensor: Device proposal and investigation," *Semicond. Sci. Technol.*, vol. 36, no. 9, Aug. 2021, Art. no. 095033.
[16] A. Goel, S. Rewari, S. Verma, S. S. Deswal, and R. S. Gupta, "Dielectric modulated junctionless biotube FET (DM-JL-BT-FET) bio-sensor," *IEEE Sensors J.*, vol. 21, no. 15, pp. 16731–16743, Aug. 2021.
[17] C. Li, F. Liu, R. Han, and Y. Zhuang, "A vertically stacked nanosheet Gate-all-around FET for biosensing application," *IEEE Access*, vol. 9, pp. 63602–63610, 2021.
[18] S. Rashid, F. Bashir, and F. A. Khanday, "Dielectrically modulated label free metal controlled organic thin film transistor for biosensing applications," *IEEE Sensors J.*, vol. 21, no. 16, pp. 18318–18325, Aug. 2021.

[19] G. Wadhwa and B. Raj, "Design, simulation and performance analysis of JLTFET biosensor for high sensitivity," *IEEE Trans. Nanotechnol.*, vol. 18, pp. 567–574, 2019.

[20] P. Venkatesh, K. Nigam, S. Pandey, D. Sharma, and P. N. Kondekar, "A dielectrically modulated electrically doped tunnel FET for application of label free biosensor," *Superlattices Microstruct.*, vol. 109, pp. 470–479, Sep. 2017.

[21] Z. Ahangari, "Performance assessment of dual material gate dielectric modulated nanowire junctionless MOSFET for ultrasensitive detection of biomolecules," *RSC Adv.*, vol. 6, pp. 89185–89191, Sep. 2016.

[22] S. K. Jain, A. M. Joshi, and A. D. Dwivedi, *Technology and Modeling of DNTT Organic Thin-Film Transistors*, 1st ed. London, U.K.: IET, 2020.

[23] T. Minamiki, T. Minami, Y.-P. Chen, T. Mano, Y. Takeda, K. Fukuda, and S. Tokito, "Flexible organic thin-film transistor immunosensor printed on a one-micron-thick film," *Commun. Mater.*, vol. 2, no. 1, p. 8, Jan. 2021.

[24] T. Zaki, S. Scheinert, I. Hörselmann, R. Rödel, F. Letzkus, H. Richter, U. Zschieschang, H. Klauk, and J. N. Burghartz, "Accurate capacitance modeling and characterization of organic thin-film transistors," *IEEE Trans. Electron Devices*, vol. 61, no. 1, pp. 98–104, Jan. 2014.

[25] S. Scheinert, T. Zaki, R. Rödel, I. Hörselmann, H. Klauk, and J. N. Burghartz, "Numerical analysis of capacitance compact models for organic thin-film transistors," *Organic Electron.*, vol. 15, no. 7, pp. 1503–1508, Jul. 2014.

[26] M. W. Alam, Z.-K. Wang, S. Naka, and H. Okada, "Top contact pentacene based organic thin film transistor with bi-layer TiO_2 electrodes," *J. Photopolymer Sci. Technol.*, vol. 25, pp. 659–664, Jun. 2012.

[27] U. Kraft, K. Takimiya, M. J. Kang, R. Rödel, F. Letzkus, J. N. Burghartz, E. Weber, and H. Klauk, "Detailed analysis and contact properties of low-voltage organic thin-film transistors based on dinaptho[2,3-b:2',3'-f]thieno[3,2-b]thiophene (DNTT) and its didecyl and diphenyl derivatives," *Org. Electron.*, vol. 35, pp. 33–40, Aug. 2016.

[28] P. Dwivedi and A. Kranti, "Dielectric modulated biosensor architecture: Tunneling or accumulation based transistor?" *IEEE Sensors J.*, vol. 18, no. 8, pp. 3228–3235, Apr. 2018.

[29] D. Gupta, N. Jeon, and S. Yoo, "Modeling the electrical characteristics of TIPS-pentacene thin-film transistors: Effect of contact barrier, field-dependent mobility, and traps," *Organic Electron.*, vol. 9, no. 6, pp. 1026–1031, Dec. 2008.

[30] A. Borodin and M. Reichling, "Characterizing TiO_2(110) surface states by their work function," *Phys. Chem. Chem. Phys.*, vol. 13, no. 34, pp. 15442–15447, Aug. 2011.

[31] B. Kumar, B. K. Kaushik, and Y. S. Negi, "Organic thin film transistors: Structures, models, materials, fabrication, and applications: A review," *Polym. Rev.*, vol. 54, no. 1, pp. 33–111, 2014.

[32] S. K. Jain, A. M. Joshi, and D. Bharti, "Performance investigation of organic thin film transistor on varying thickness of semiconductor material: An experimentally verified simulation study," *Semiconductors*, vol. 54, no. 11, pp. 1483–1489, Nov. 2020.

[33] G. Wadhwa and B. Raj, "Label free detection of biomolecules using charge-plasma-based gate underlap dielectric modulated junctionless TFET," *J. Electron. Mater.*, vol. 47, no. 8, pp. 4683–4693, May 2018.

[34] D. Singh, S. Pandey, K. Nigam, D. Sharma, D. S. Yadav, and P. Kondekar, "A charge-plasma-based dielectric-modulated junctionless TFET for biosensor label-free detection," *IEEE Trans. Electron Devices*, vol. 64, no. 1, pp. 271–278, Jan. 2017.

[35] E. Rahman, A. Shadman, and Q. D. M. Khosru, "Effect of biomolecule position and fill in factor on sensitivity of a dielectric modulated double gate junctionless MOSFET biosensor," *Sens. Bio-Sensing Res.*, vol. 13, pp. 49–54, Apr. 2017.

[36] A. Kumar, M. Roy, N. Gupta, M. M. Tripathi, and R. Chaujar, "Dielectric modulated transparent gate thin film transistor for biosensing applications," *Mater. Today, Proc.*, vol. 28, no. 1, pp. 141–145, Jan. 2020.

[37] S. A. Hafiz, Iltesha, M. Ehteshamuddin, and S. A. Loan, "Dielectrically modulated source-engineered charge-plasma-based Schottky-FET as a label-free biosensor," *IEEE Trans. Electron Devices*, vol. 66, no. 4, pp. 1905–1910, Apr. 2019.

[38] A. Joshi, "Label-free detection of biomolecules using dielectric-modulated top contact bi-layer electrodes organic thin film transistor," TechRxiv, Apr. 2022, doi: 10.36227/techrxiv.19622469.v1.

SUSHIL KUMAR JAIN received the master's degree from the Malaviya National Institute of Technology (MNIT), Jaipur (one of the prestigious institutes in India), where he is currently pursuing the Ph.D. degree. He has a total of ten years of experience in teaching and in the industry. His current research interest includes modeling and simulation of organic thin film transistors (OTFTs).

AMIT MAHESH JOSHI (Senior Member, IEEE) received the M.Tech. and Ph.D. degrees from NIT, Surat, in 2009 and 2015, respectively. He has been an Assistant Professor with the Malaviya National Institute of Technology Jaipur (MNIT Jaipur), since July 2013. He has published more than 100 research articles in excellent peer-reviewed international journals/conferences and eight book chapters. He has 1094 Google scholar citations, i10 index is 35, and H-index is 17. His area of specialization is biomedical signal processing, smart healthcare, VLSI DSP systems, and embedded system design. He is a member of IETE and ACM. He served as a Technical Program Committee Member for IEEE Conferences (iSES, ICCE, ISVLSI, and VDAT). He received the honor of a UGC Travel Fellowship, the SERB DST Travel Grant Award, and the CSIR Fellowship. He has attended well-known IEEE Conferences, such as TENCON-16, TENCON-17, ISCAS-18, and MENACOMM-19. He has also served as a Mentor for IEEE Engineering in Medicine and Biology Society Student Mentorship Program 2021. He has supervised three Ph.D. theses, and one more research scholar has submitted their thesis. He has also supervised 23 M.Tech. projects and 17 B.Tech. projects in biomedical signal processing and VLSI/embedded systems. He was a Reviewer of technical journals, such as IEEE TRANSACTIONS/IEEE ACCESS, Springer, and Elsevier.

LINGA REDDY CENKERAMADDI (Senior Member, IEEE) received the master's degree in electrical engineering from the Indian Institute of Technology Delhi (IIT Delhi), New Delhi, India, in 2004, and the Ph.D. degree in electrical engineering from the Norwegian University of Science and Technology (NTNU), Trondheim, Norway, in 2011.

He worked with Texas Instruments on mixed-signal circuit design before joining the Ph.D. Program at NTNU. After finishing the Ph.D. degree, he worked on radiation imaging for an atmosphere–space interaction monitor (ASIM mission to the International Space Station) with the University of Bergen, Bergen, Norway, from 2010 to 2012. He is currently a Leader of the Autonomous and Cyber-Physical Systems (ACPS) Research Group and a Professor with the University of Agder, Grimstad, Norway. He has coauthored over 130 research publications that have been published in prestigious international journals and standard conferences in the research areas of the Internet of Things (IoT), cyber-physical systems, autonomous systems, robotics and automation involving advanced sensor systems, computer vision, thermal imaging, LiDAR imaging, radar imaging, wireless sensor networks, smart electronic systems, advanced machine-learning techniques, connected autonomous systems, including drones/unmanned aerial vehicles (UAVs), unmanned ground vehicles (UGVs), unmanned underwater systems (UUSs), 5G- (and beyond) enabled autonomous vehicles, and socio-technical systems, such as urban transportation systems, smart agriculture, and smart cities. He is also quite active in medical imaging.

Dr. Cenkeramaddi is a member of ACM and a member of the editorial boards of various international journals and the technical program committees of several IEEE conferences. He serves as a reviewer for several reputed international conferences and IEEE journals. Several of his master students won the Best Master Thesis Awards in information and communication technology (ICT). He is the Principal Investigator and a Co-Principal Investigator of many research grants from the Norwegian Research Council.